

Multibandgap quantum well wafers by IR laser quantum well intermixing: simulation of the lateral resolution of the process

Oleksandr VOZNYI, Radoslaw STANOWSKI and Jan J. DUBOWSKI

*Department of Electrical and Computer Engineering
Research Center for Nanofabrication and Nanocharacterization
Université de Sherbrooke, Sherbrooke, Québec J1K 2R1, Canada
E-mail: jan.j.dubowski@usherbrooke.ca*

Post-growth selective-area bandgap tuning of quantum well (QW) microstructures has been investigated using Finite Element Method computer simulations. Laser fast scanning is proposed as a way to overcome the problem of damaging the surface with a small spot needed to obtain better spatial resolution. Influence of laser parameters, background heating, beam scanning speed and properties of QW microstructures on the ability to achieve sharp bandgap profiles in the laser-written intermixed material are investigated. Lateral resolution of 2 μm is expected to be achievable with a 12- μm beam laser rapid thermal annealing.

Keywords: quantum well intermixing, laser rapid thermal annealing, monolithically integrated devices, modeling wafer level processing, direct bandgap engineering, semiconductor micro- and nano-structures

1. Introduction

Post-growth selective-area bandgap tuning of quantum well (QW) microstructures is an attractive approach to fabricate monolithically integrated photonic devices. Bandgap tuning can be achieved by implanting ions through special masks and, subsequently, by rapid thermal annealing (RTA) leading to selective area quantum well intermixing (QWI). Direct irradiation with a focused IR laser beam could also be used to achieve a similar effect in a much simplified manner. We have already demonstrated that an array of 12 lines of the GaAs/AlGaAs QWI material can be 'written' by fast scanning a 0.6 mm-wide beam of a CW Nd:YAG laser [1]. Our earlier results have also demonstrated the successful use of a CW Nd:YAG laser for writing 100 μm -wide lines of the QWI material in InP/GaInAs [2]. Lines 25 and 0.19 μm wide of the material intermixed by laser annealing have also been reported in literature [3, 4].

The process of laser-QWI remains to be poorly understood and insufficient evidence, both experimental and theoretical, has been available to illustrate its reproducibility and/or the ultimate lateral resolution.

In this paper, we investigate the influence of laser parameters, power deposition rate and properties of QW microstructures on the ability to achieve sharp bandgap profiles in the laser-written QWI material.

We demonstrate that a significant improvement of the lateral resolution can be obtained if the intermixing is carried out with a laser beam which power, diameter and scanning speed are properly matched with the size and shape of the processed wafer as well as with the required bandgap engineered pattern.

2. Computation details

Calculations have been carried out for a QW laser structure grown on InP ($E_g=1.35$ eV) and consisted of

8.5-nm InGaAs wells ($E_g=0.72$ eV) with 12-nm InGaAsP barriers ($E_g=0.98$ eV). The active region was bound by a 130-nm InGaAsP stepped graded index (GRIN) ($E_g=1.05 - 1.18$ eV) layer and a 1.4- μm -thick doped InP cap layer. We used experimental data of bandgap shifting during RTA for such a microstructure [3] as the input data in our calculations.

2.1 Modeling of temperature profiles

Simulations have been carried out using the heat transfer module of commercial finite element software (FEMLAB), which is suitable for both stationary and transient heat flow calculations. We assumed that epitaxially grown QW layers, which have different heat conduction properties than those of InP, are sufficiently thin and therefore the calculations could be carried out for pure InP.

We carried out full 3D calculations, which enabled us to provide more accurate lateral temperature profiles, to provide important information about in-depth heat distribution and to describe the results achieved with a moving laser beam. Background heating was modeled to be achieved with a large diameter flat top laser beam instead of an infinite heat sink. Heat losses due to convection in the air and radiation were also taken into account. Our model was tested to successfully describe experimental results of laser heated Si and GaAs wafers [5]. We also were able to correctly describe PL shift profiles observed in [1] for a GaAs/AlGaAs sample irradiated with a 0.6 mm-wide moving laser beam.

Parameters used in the calculations are compiled in Table 1. The density of InP changes less than 3% in the temperature range of interest and we assumed it to be constant. Temperature dependent specific heat C_p was included in the calculations, although, it appears that due to the weak temperature dependence of this coefficient (it

Table 1 Material parameters of InP used in calculations

Specific heat, C_p	410 (at 300K) – 455 (at 1000K) J/kg·K (Ref. [10])
Density, ρ	4810 kg/m ³
Thermal conductivity, k	216800·T ^{-1.45} W/m·K (Ref. [3])
Reflectivity, R	0.1
Convection coefficient, h	20 W/K·m ²
Absorption, α	10 ⁵ cm ⁻¹
Emissivity, ε	0.7

changes from 410 J/kg·K at 300 K to 455 J/kg·K at 1000 K [10]) such an approach has a negligible effect on the accuracy of calculations.

Our simulations showed the importance of using the temperature dependent thermal conductivity coefficient. The value of k at 1000 K is 5 times smaller than at room temperature [3, 10], which results in slower heat dissipation at elevated temperatures and, consequently, in higher temperatures induced by the laser beam.

We assumed that a protective SiO₂ layer was used to prevent the laser-irradiated surface from decomposition. Such a layer also acts as an antireflection coating reducing the overall wafer reflectivity [5]. The generation of vacancies induced by the SiO₂ cap, which is known to promote interdiffusion, has not been taken into account.

It has been argued [3] that the 1064 nm photoabsorption-induced QWI should be considered QW microstructure composition dependent because InP is practically transparent at that wavelength. In practice, this in fact does not take place. To achieve the temperatures needed for intermixing with the laser energy absorbed only in a QW layer, one would require power densities exceeding the known values of surface damage for this material [11]. The mechanism of heating a semiconductor wafer with a high-power laser can be described as a 2-step process [11,12]. Firstly, the high-power laser beam induces an avalanche generation of carriers in the surface region (dopants and/or multi-phonon absorption serve as a source of initial free carriers). Secondly, the excited surface region will more efficiently absorb laser energy and then transfer it to the lattice by Auger and surface recombination. After preheating the surface region to temperatures at which the semiconductor bandgap is comparable or smaller than the laser photon energy (approximately 500°C for InP irradiated with an Nd:YAG laser), the bulk absorption will add to the process. For temperatures higher than 500°C the bulk absorption of InP reaches 10⁴-10⁵ cm⁻¹ [7,8], which means that the absorption depth is 0.1-1 μm. Our experiments [5] confirm the possibility of heating a semi-insulating GaAs wafer to high temperatures in several seconds with a 1 W/mm² laser beam. This is impossible if one assumes that absorption is equal to its bulk value of $\alpha=30$ cm⁻¹. Thus, all the laser energy is absorbed in a thin

region at the surface of the InP capping layer, and it is transferred inside of the material only by heat conduction. Consequently, we used surface absorption instead of volume absorption in our calculations. This approach also allowed us to significantly reduce the calculation time. Moreover, we verified that the temperature distribution in-depth of the wafer does not change significantly if the absorption coefficient reaches 1000 cm⁻¹ or greater values.

Due to complexity of experimental measurements of emissivity, there are significant discrepancies in the estimated emissivity of InP reported in literature [13-15]. Nevertheless, it is widely assumed that for non-transparent wafers (which is the case for InP starting from 500°C) the emissivity reaches its maximum value. Following the similarities of InP and GaAs emissivity values [13] and considering the temperature dependence of the emissivity for GaAs [14], we use the value $\varepsilon=0.7$ for the whole range of temperatures.

It was found that the results obtained using constant, high temperature values of thermal conductivity, optical absorption and emissivity coefficients differ no more than 2% from the results obtained with temperature dependent coefficients.

2.2 Diffusion coefficient

In order to relate thermal distribution to the intermixing profile, the thermal dependence of the disordering rate must be quantified. Photoluminescence (PL) data after RTA at different temperatures [3] were used for this purpose. Since temperature and anneal times are predetermined and the material parameters are known, diffusion coefficients can be calculated.

Assuming the diffusion coefficient as a parameter, one needs to solve the diffusion equation and calculate the concentration profiles for a given annealing time. For constant temperature conditions, such as those achieved with RTA, concentration profiles can be represented by a superposition of error functions [9]. For temperatures varying with time, the diffusion equation should be solved numerically. This was accomplished with FEMLAB. We assumed one single diffusion coefficient for all atomic species, i.e., conservation of the lattice matching after annealing [9].

Schrödinger's equation has to be solved for the QW to determine the energy levels for electrons and holes and the resulting PL wavelengths. These simulations were also carried out in FEMLAB using the values of bandgaps, effective masses, band offsets and bandgap bowings from [6,9].

Using the calculated relation of PL wavelength shift vs. diffusion coefficient and experimental data of PL shift for different anneal temperatures (for the same annealing time as in calculations) [3], we can find the diffusion coefficients for given anneal temperatures. Then, from the Arrhenius plot of $\ln(D)$ as a function of $1/kT$ it is possible to find the temperature dependent diffusion coefficient:

$$D = D_0 \exp(-E_A/kT) \quad (1)$$

Our calculated values of the constants for InP are $D_0=9.1 \cdot 10^{-11}$ m²/s and $E_A=1.98$ eV, which is in reasonable agreement with those values obtained in [3]. Once all

constants are known, it is possible to calculate the PL shift of the material for any time and temperature.

Although calculations for the RTA results of QWI InGaAs/InGaAsP had already been carried out [3], and the calculated relation between PL shift and diffusion coefficient could be used to obtain PL shift for any given temperature profile constant with time, one needs to solve the diffusion equation and then Schrödinger's equation from scratch to obtain the PL shift profile for temperature profiles varying with time. Thus, we reproduced the model to be able to calculate PL shift profiles for a moving laser beam.

3. Results

3.1 Power density

Fig. 1a shows the calculated laser beam power needed to heat a 2-inch InP wafer to a given temperature using a 0.1 mm laser spot. As one can see from Fig. 1b, much higher power densities are required to achieve the same temperatures with a smaller laser beam. This can be explained by more efficient heat dissipation through thermal conductivity in the wafer irradiated with a small laser beam. Although such power densities don't induce melting (these have often been used to define surface damage threshold [11, 12]), it would still be desirable to experimentally verify whether they would damage the surface. Another factor that can cause surface damage is thermal stress resulting from significant temperature gradients. Background heating can be used as a way to reduce both temperature gradients and the input laser power.

Scanning of the laser beam can also be used to overcome the problem of damaging the surface with small spots. As one can see from Fig. 1, the power needed to heat the wafer to the target temperature increases with the scanning speed. However, this is compensated for by the significantly decreased laser dwell time. For instance, for the 12- μm beam scanned at 5 cm/s the dwell time is only 0.2 ms. It is reasonable to expect that this would allow to the carrying out the irradiation with significantly increased fluences while avoiding damage to the surface.

3.2 Temperature profiles

Calculated temperature profiles for 100 μm and 12 μm beam diameters and different background temperatures are shown in Fig. 2. The input power for every simulation has been adjusted to reach the maximum temperature of 1073 K. This value was chosen as it is known to cause a PL shift of approximately 100 nm for a 90-s anneal in a RTA furnace [3].

As was noted earlier, due to full laser beam energy absorption at the surface, heat propagates inside the wafer by heat conduction only. That is why the material is heated to high temperatures only inside a small semi-sphere with a radius comparable to the beam radius, with temperature decreasing very quickly with depth. This would result in a reduced intermixing resolution and much longer annealing time required to achieve the needed PL shift for typical quantum well layers that are usually situated at about 2- μm depth.

It can be seen in Fig. 2b that for the 12- μm beam the temperature at 2 μm below the surface is much lower than needed for intermixing. Background heating can significantly increase the temperature below the surface for the 100- μm beam, but for the 12- μm beam diameter, even with background heating, the temperature induced at a depth greater than 2 μm would not be sufficient to induce QWI.

Our simulations showed that for large enough samples the temperature profiles do not depend on scanning speed, i.e., temperature distribution in the plane perpendicular to scanning direction, at the moment when the laser beam center passes this plane, will be the same as for the stationary beam (assuming that laser power is adjusted to achieve the same maximum temperature).

For small samples (with linear dimensions up to 100 times bigger than the laser beam diameter) the absorbed laser energy cannot dissipate fast enough through convection and radiation. This will result in an increasing sample background temperature until some steady-state condition has been reached. In such a case, different temperature profiles can be expected for moving laser beams when compared to those induced with stationary laser beams. Generally, for small samples, especially at

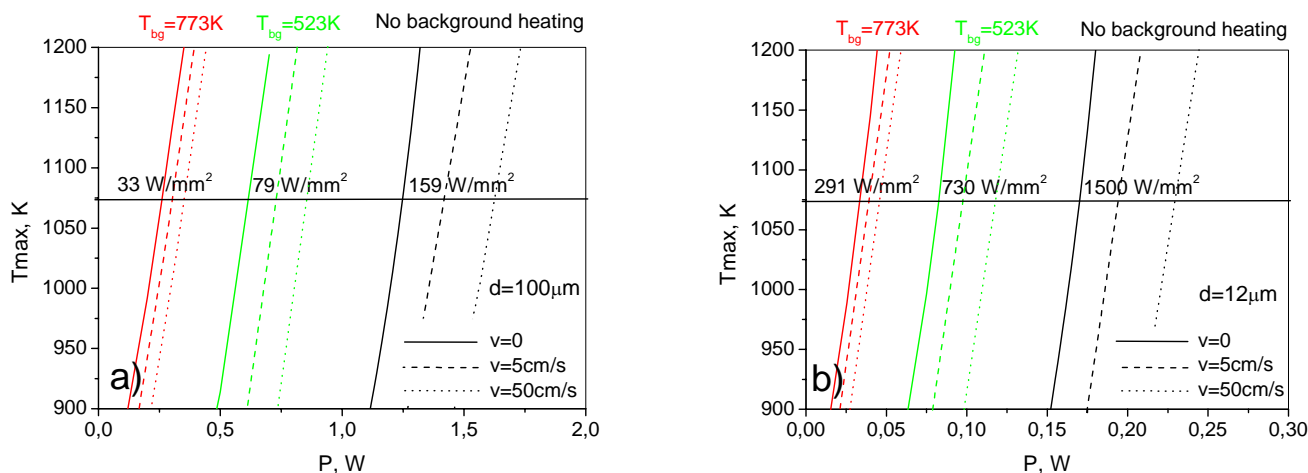


Fig. 1 Dependence of InP sample surface temperature in the center of the beam (T_{max}) on laser power for different scanning speeds and for beam diameters of 100 μm (a) and 12 μm (b). Power densities needed to achieve 1073 K with a stationary beam are shown in the picture. Horizontal line – temperature giving 100 nm PL shift in the InGaAs/InGaAsP QW microstructure following the 90-s RTA [3].

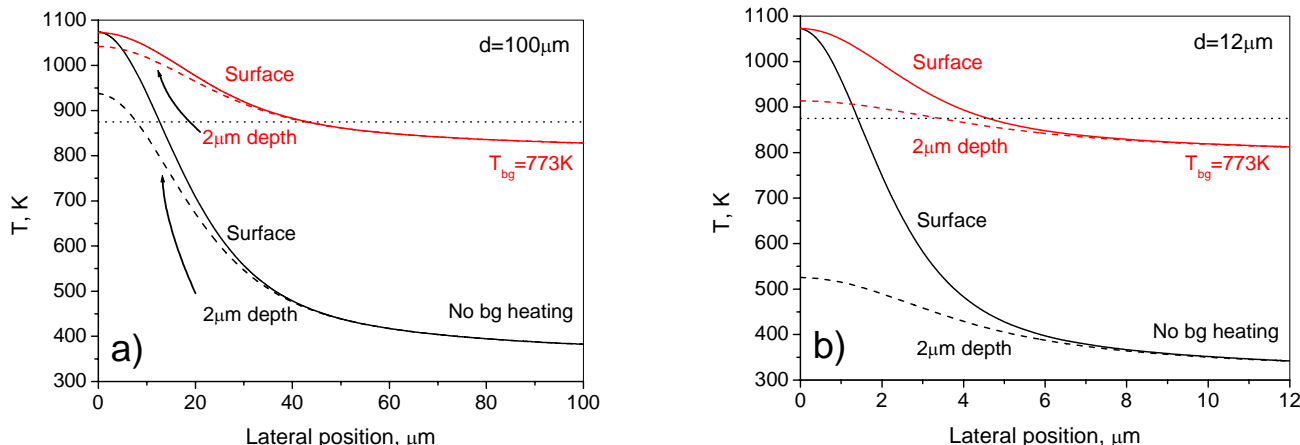


Fig. 2 Calculated temperature profiles on the surface and 2 μm below the surface for a 2-inch InP wafer irradiated by laser beams of 100 μm (a) and 12 μm (b) diameters. Laser power was adjusted for every simulation to reach the same maximum temperature. Horizontal line indicates the threshold temperature for which a 90-sec RTA induces no significant PL shift [3].

slow scanning speeds, the background temperature will increase even for a moving beam. This will result in increasing the maximum temperature induced from scan to scan. To achieve better control over the intermixing process and predictable results for small samples, it is important to choose the regime where induced temperature profiles during each scan will be equivalent. This can be achieved, for example, by choosing a longer pause between scans thereby allowing the sample to cool down to the previous background temperature.

3.3 PL shift profiles

Having determined the functional form of PL shift dependence on diffusion coefficient and time, we can easily calculate the disordering (intermixing) profile for any given temperature profile. To find the PL shift profile for a moving laser beam we need to determine the temporal behavior of temperature at different distances from the center of the laser line, and then solve the diffusion equation. This will allow us to find the concentration profile induced with a defined number of scans. In the next step, we solve the Schrödinger's equation to find PL at every point near the scan line. As can be seen in Fig. 3, temperature in the proximity of a point crossed by the

scanning laser beam increases/decreases rapidly as the beam approaches/leaves that point. This can be compared to pulse heating of the sample. For the case of a 2-inch wafer, its temperature differs from the initial value only during the dwell time, which is about 2 ms for 100- μm spot scanned at 5 cm/s. This means that any point on the wafer doesn't really 'feel' what happens in other points.

Note that the temperature at the 15- μm distance from the line center never reaches the value needed for intermixing. Thus, we can expect that the width of the intermixed line written with the 100- μm spot would be less than 30 μm .

We should also note that the normalized temperature temporal profile practically doesn't depend on the scanning speed and beam size, except that for 100- μm beam and speeds below 5 cm/s it widens a little due to an increase of the background temperature of the wafer by about 50 K.

The calculated PL shift profiles for processing with the 12- μm laser spot which was either stationary ($v=0$) or moving at $v=50\text{ cm/s}$ are shown in Fig. 4. The exponential dependence of the shift on temperature results in a rather narrow disordered region, the sharpness of which generally depends on the diffusion activation energy of the material. Due to different temporal behaviors of temperature profiles

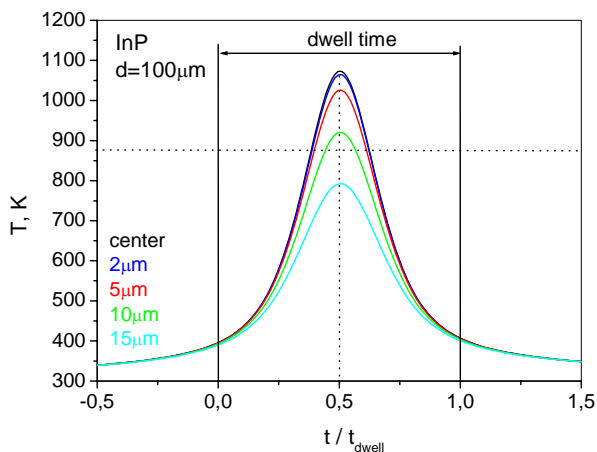


Fig. 3 Temperature temporal profile in the center of the laser scanned line and at different distances from its center.

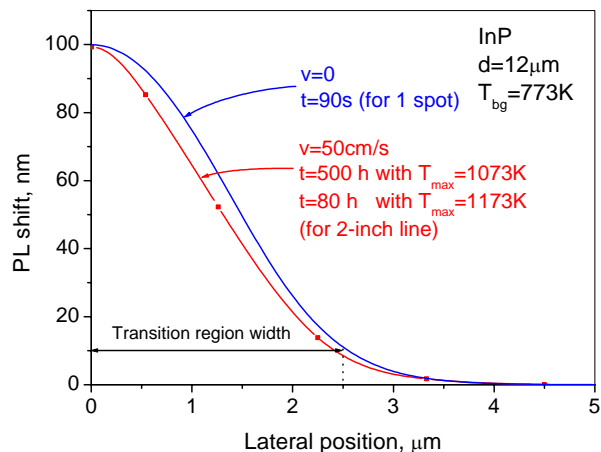


Fig. 4 Calculated intermixing profiles for different scanning speeds.

for $v = 0$ and 50 cm/s, PL shift profiles are not exactly the same, but the resolution of the intermixing process is comparable. It can be seen that a 5- μm wide line of the 100-nm shifted GaInAs/GaInAsP QW material is predicted to be achievable with a 12- μm diameter laser beam and background heating to 773 K.

Of particular importance is that the shape of the PL shift profile doesn't depend on the maximum temperature in the wafer. Fig.5 shows temperature profiles for different laser beam powers, but with the same beam diameter and background heating conditions as used for the calculation of data presented in Fig. 4. These curves are almost parallel, which means that the ratio of diffusion coefficients for given temperature profiles in any lateral position is constant. Clearly, the same intermixing results can be achieved with shorter anneal times at higher temperature as those at lower temperature but with proportionally longer anneal times. For example, a presented difference of 100 K in Fig. 5 results in a 2.5 times higher maximum value of the PL shift. PL shifts obtained with high-power irradiation in that case could be reproduced with the low-power irradiation if the anneal time was 6 times longer.

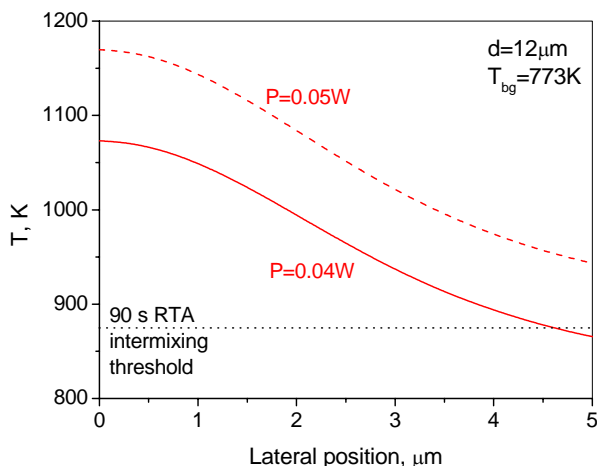


Fig. 5 Temperature profiles induced by laser beams of different power.

3.4 Processing time

To quantitatively describe the resolution of intermixing, we define the transition region width as the lateral distance between the maximum and 10% values of the PL shift.

Fig. 6 summarizes the results of calculations for 100 and 12 μm beam diameters and different background temperatures. It can be seen that the PL shift resolution at 2- μm depth for the 100 μm beam does not differ significantly from its value at the surface. However, up to 3-fold widening of the transition region has been expected for irradiation with a 12- μm beam. For QWs located 2 μm below the surface, the time needed to achieve a 100 nm bandgap shift with a stationary beam is 750 s. The processing time for writing a 2-inch long line of the 100-nm shifted material is about 50 hours, assuming the sample background temperature is maintained at 773 K. Shorter annealing times would require QWs to be located closer to the surface and/or processing with a larger diameter laser beam. In our calculations, we used $T_{\text{max}}=1173$ K, just because it is known to produce a 100 nm

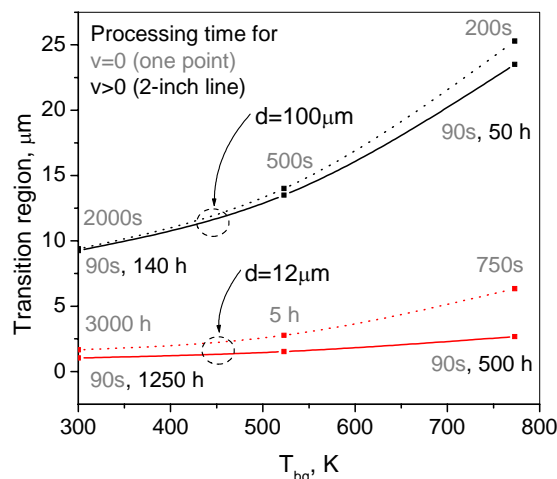


Fig. 6 Transition widths and processing times to write a 2-inch line of the 100 nm bandgap shifted material at $T_{\text{max}} = 1073$ K. The results at the surface (solid line) and 2 μm below the surface (dotted line) have been calculated for 100 and 12 μm beam diameters as a function of the background temperature.

PL shift for 90-s RTA. With higher maximum temperatures the annealing time could be further reduced. Also, the size of devices created with intermixed material is only several millimeters, so the overall time to fabricate one device could be much shorter. Finally, the 100-nm PL shift will probably not be needed for all applications. Decreasing the final value of the shift by 5 times will decrease processing time by about 25 times.

4. Conclusions

Laser rapid thermal annealing (LRTA), based on irradiation with a CW laser beam, has been investigated on an example of the InGaAs/InGaAsP QW microstructure as a promising quantum-well intermixing technique for bandgap tuning of III-V materials. The technique has the potential to write the QWI material with a lateral resolution of about 2 μm (assuming 12- μm laser beam, no background heating and QW situated very close to the surface). This is comparable to the resolution achieved with pulsed laser or ion-implantation QWI techniques. Albeit, writing a line of the intermixed material with a 12- μm laser beam would take too much time and bigger beam diameters should be probably used, leading to a resolution of about 20-50 μm . However, unlike other methods of QWI, the LRTA is a one-step process, which offers the means to achieve targeted values of intermixing (bandgap shifting) with precision likely unattainable by other methods. In addition, this technique can be used to write almost arbitrary shape lines of the QWI material.

Undertaken simulations provide an understanding of the process and give some guidelines on how to achieve the best resolution and short processing times:

1. Scanning speed can be used to adjust the fluence below damage threshold without compromising the lateral resolution of the QWI process.
2. To reduce processing time, QWs should be very close to the heated surface, and the maximum temperature should be as high as allowed by the material decomposition temperature.

3. Background heating can be used to further decrease the processing time (especially for deep QWs) or to decrease the input power density, but it also causes a decrease in the resolution.

Acknowledgments

The funding for this research was provided by the Natural Sciences and Engineering Research Council of Canada and the Canada Research Chair Program.

References

- [1] J. J. Dubowski, C. Y. Song, J. Lefebvre, Z. Wasilewski, G. Aers, and H. C. Liu: *J. Vac. Sci. Technol. A*, **22**, (2004) 887.
- [2] J. J. Dubowski, C. Lacelle and M. Buchanan: *Proc. SPIE*, **3274**, (1998) 53.
- [3] A. McKee, C. J. McLean, G. Lullo, A. C. Bryce, R. M. De La Rue, J. H. Marsh, and C. C. Button: *IEEE J. Quant. Electron.*, **33**, (1997) 45.
- [4] M. K. Kelly: *Appl. Phys. Lett.*, **68**, (1996) 1984.
- [5] R. Stanowski, O. Voznyy, and J. J. Dubowski: *J. Laser Micro/Nanoengineering*, this issue.
- [6] I. Vurgaftman, J. R. Meyer, and L. R. Ram-Mohan: *J. Appl. Phys.*, **89**, (2001) 5815.
- [7] W. J. Turner, W. E. Reese, and G. D. Pettit: *Phys. Rev.*, **136**, (1964) A1467.
- [8] D. E. Aspnes and A. A. Studna: *Phys. Rev. B*, **27**, (1983) 985.
- [9] H. Peyre, F. Alsina, J. Camassel, J. Pascual, and R. W. Glew: *J. Appl. Phys.*, **73**, (1993) 3760.
- [10] V. Palankovski, R. Schultheis, S. Selberherr: *IEEE Transactions On Electron Devices*, **48**, (2001) 1264.
- [11] A. V. Kuanr, S. K. Bansal, G. P. Srivastava: *Optics & Laser Technol.*, **28**, (1996) 25.
- [12] M. Lenzner: *International Journal of Modern Physics B*, **13**, (1999) 1559.
- [13] T. Mizutani: *J. Vac. Sci. Technol. B*, **6**, (1988) 1671.
- [14] A. S. Jordan: *J. Appl. Phys.*, **51**, (1980) 2218.
- [15] P. J. Timans: *J. Appl. Phys.*, **72**, (1992) 660.

(Received: April 21, 2005, Accepted: November 1, 2005)